Solar Energy Materials & Solar Cells ▮ (▮▮▮▮) ▮▮▮–▮▮▮

Contents lists available at ScienceDirect

Solar Energy Materials & Solar Cells

journal homepage: www.elsevier.com/locate/solmat

# Microcrystalline and micromorph device improvements through combined plasma and material characterization techniques

G. Bugnon [a,*], A. Feltrin [a], R. Bartlome [a], B. Strahm [a], A.C. Bronneberg [b], G. Parascandolo [a], C. Ballif [a]

[a] Ecole Polytechnique Fédérale de Lausanne (EPFL), Photovoltaics and Thin Film Electronics Laboratory, Rue A.-L. Breguet 2, CH-2000 Neuchâtel, Switzerland
[b] University of Technology of Eindhoven, P.O. Box 513, 5600 MB Eindhoven, The Netherlands

ARTICLE INFO

*Article history:*
Received 5 November 2009
Received in revised form
19 February 2010
Accepted 4 May 2010

*Keywords:*
Solar cell
Microcrystalline silicon
Intrinsic stress

ABSTRACT

Hydrogenated microcrystalline silicon ($\mu c$–Si : H) growth by very high frequency plasma-enhanced chemical vapor deposition (VHF-PECVD) is studied in an industrial-type parallel plate KAI reactor. Combined plasma and material characterization techniques allow to assess critical deposition parameters for the fabrication of high quality material. A relation between low intrinsic stress of the deposited *i*-layer and better performing solar cell devices is identified. Significant solar cell device improvements were achieved based on these findings: high open circuit voltages above 520 mV and fill factors above 74% were obtained for 1 μm thick $\mu c$–Si : H single junction cells and a 1.2 $cm^2$ micromorph device with 12.3% initial ($V_{oc}$ = 1.33 V, FF = 72.4%, $J_{sc}$ = 12.8 mA $cm^{-2}$) and above 10.0% stabilized efficiencies.



## 1. Introduction

Despite the strong potential for industrial applications of $\mu c$–Si : H material in highly efficient multi-junction solar cell devices, mainly because of its enhanced absorption in the infrared (IR) and robustness to light-induced degradation, the deposition conditions by PECVD favoring device grade $\mu c$–Si : H material quality have yet to be fully understood. The crucial roles of atomic hydrogen and ion bombardment for determining the Si:H film microstructure has commonly been accepted. As device grade material is typically found in the *a*-Si:H to $\mu c$–Si : H transition it is of practical interest to understand the underlying mechanisms allowing this phase change. In particular, it has been identified that for $\mu c$–Si : H nucleation to occur, the hydrogen atom flux to silicon precursor flux ratio toward the growing surface has to exceed a certain threshold value. For this condition to be fulfilled numerous plasma deposition parameters can be adjusted. However silane concentration in the plasma, which is a function of silane depletion, was identified as a determining factor for reaching this microstructure transition [1]. High intrinsic stress within the *a*-Si:H phase was also found to be a prerequisite for nucleation [2]. Ultimately the defect density of the deposited material will also limit the performance of the solar cells. In addition, because of the thick $\mu c$–Si : H active layer requirement, typically above 1 μm, high deposition rates while retaining high material quality are desirable.

In this study, VHF-PECVD was used in an industrial-type reactor, where combined plasma diagnostic techniques and thin film material characterizations were used to identify some critical deposition parameters necessary to obtain low stress $\mu c$–Si : H material, and its relation with better performing solar cells when used as an absorber layer.

## 2. Experimental details

### 2.1. PECVD system and plasma diagnostic techniques

A medium-sized version of the large area industrial KAI™ systems [3] was used to deposit all the $\mu c$–Si : H layers and solar cells contained in this study. The dimensions of the Plasmabox are 50 × 60 $cm^2$, inter-electrode distance was set to 13 mm, the generator frequency to 40.68 MHz and the deposition temperature was fixed at 180 °C. Silane dissociation efficiency ($D$) was evaluated by tunable IR laser spectrometry, allowing the analysis of rotovibrational absorption lines of silane directly through the exhaust line of the deposition system [4]. This allows for the estimation of silane concentration in the plasma ($c_p$) and film growth rate estimations. Powder formation was diagnosed using laser light scattering in the visible. Time-resolved optical emission spectroscopy (OES) was also used as a non-intrusive diagnostic technique [5,6]. Emission intensities from the $H_2$ Fulcher (600–630 nm) and $G_0B_0$ (461–464 nm) were integrated to evaluate their ratio $I_{G_0B_0}/I_{Ful}$ which allows us to check $T_e$ variation over time, and in particular from ignition to steady-state equilibrium.

* Corresponding author. Tel.: +41 32 718 33 41; fax: +41 32 718 32 01.
*E-mail address:* gregory.bugnon@epfl.ch (G. Bugnon).

0927-0248/$ - see front matter © 2010 Elsevier B.V. All rights reserved.
doi:10.1016/j.solmat.2010.05.014

SiH* emission (409–423 nm), originating from electron impact $SiH_4$ excitation, along with proper $H_2^*$ background subtraction, was used to get silane density information in the plasma.

### 2.2. Material and solar cell device characterization

Layers were always co-deposited on both Schott AF45 glass and Si-wafer to analyze their properties. Micro-Raman spectroscopy was used to estimate the crystalline volume fraction $R_c$ of the $\mu c-$Si : H layers on glass [7], using the emission line of an $Ar^+$ laser at 514 nm. Special care was taken to always have comparable $R_c$ on glass, between 55% and 60%. Spectral ellipsometry (SE) measurements were conducted over a wide energy range (0.6–6.0 eV) with a phase-modulated spectroscopic ellipsometer to assess precisely the film thickness and composition on both type of substrates systematically.

Thicker films were also deposited on single side polished *c*-Si wafer for Fourier transform infrared spectroscopy (FTIR) to get chemical bonding information. This analysis was rendered quite difficult as only thin $\mu c-$Si : H films of around 600 nm could be deposited for the purpose of comparison, as they would immediately peel off with increased thickness when prepared at high power density. This will be discussed more in details in the next section.

Stress measurements were carried out for $\mu c-$Si : H layers deposited on Si(1 0 0) wafer strips of $50\times8\times0.3\,mm^3$ with a surface profiler. Intrinsic stress in the film $\sigma$ was calculated using

$$\sigma = Ed_s^2/[6R(1-v)d_f], \quad (1)$$

with $R$ the radius curvature, approximated here as $R=L^2/8B$ with the wafer strip length $L$ and bow height $B$ (as $L\gg B$), $E$ the silicon Young's modulus, $v$ the Poisson's ratio, $d_s$ the substrate thickness and $d_f$ the deposited film thickness [8]. The ratio $E/(1-v)$ value was taken as 180.5 GPa as reported in [9] for Si(1 0 0). Based on the uncertainties in determination of $L$, $B$ and $d_f$, we estimated the error for total stress to be within 20 Mpa.

Standard *p-i-n* solar cells were prepared to evaluate the $\mu c-$Si : H material quality when used as an absorber layer of approximately 1 μm. The back and front contacts were textured zinc oxide (ZnO) obtained through a modified low-pressure chemical vapor deposition (LPCVD) process developed at IMT [10]. The back contact is also covered with a white dielectric reflector. Open circuit voltage ($V_{oc}$) and fill factor (FF) values were derived from current-voltage curves, obtained using a Wacom AM1.5 solar simulator, and short circuit current densities ($J_{sc}$) from external quantum efficiency (EQE) measurements.

## 3. Results and discussion

### 3.1. Solar cell performances

A RF power series for the deposition of the $\mu c-$Si : H intrinsic material was done at a pressure of 3.5 mbar. Silane flow ($\Phi_{SiH_4}$) was adjusted for all the cells to keep comparable $R_c$ of about 60% within the i-layer for all regimes (see Table 1). A high silane dilution in hydrogen ($\Phi_{H_2}/\Phi_{SiH_4}$) between 33 and 40 was used here to minimize powder formation. Laser light scattering and silane depletion measurements could confirm that no powder is detected and that all silane dissociated in the plasma contributes to the film growth. Despite these process conditions, usually considered favorable for the deposition of high quality $\mu c-$Si : H material, an important deterioration of all *p-i-n* solar cell parameters has been observed by simply increasing the power density ($P_d$) from only 0.05 W cm$^{-2}$ to 0.10 W cm$^{-2}$ and 0.15 W cm$^{-2}$, with efficiencies going from 7.5%, to 6.3% and 5.0% respectively. Open circuit voltage dropped from 510 to 410 mV, fill factors from 72% to 63% and short circuit current from 20.4 to 19.4 mA cm$^{-2}$ upon slightly increasing the silane dissociation and deposition rate from 1.4 to 2.5 Å s$^{-1}$, corresponding to low silane depletion fractions between 23% and 34%. As already stated the pressure has a relatively high value of 3.5 mbar, and such deterioration can hardly be explained with increased mean ion energy.

**Table 1**
Summary of the different *i*-layers deposition conditions used for solar cells and structural characterization.

| $P_d$ (W cm$^{-2}$) | $p$ (mbar) | $\Phi_{SiH_4}$ (sccm) | $\Phi_{H_2}$ (slm) | $D$ (%) | $c_p$ (%) | GR (Å s$^{-1}$) |
|---|---|---|---|---|---|---|
| 0.05 | 3.5 | 50 | 2.0 | 22.9 | 1.9 | 1.4 |
| 0.10 | 3.5 | 53 | 2.0 | 32.5 | 1.7 | 1.8 |
| 0.15 | 3.5 | 60 | 2.0 | 34.3 | 1.9 | 2.5 |
| 0.10 | 3.5 | 32 | 0.8 | 54.6 | 1.7 | 2.0 |
| 0.15 | 7.0 | 43 | 2.5 | 41.5 | 1.0 | 3.7 |

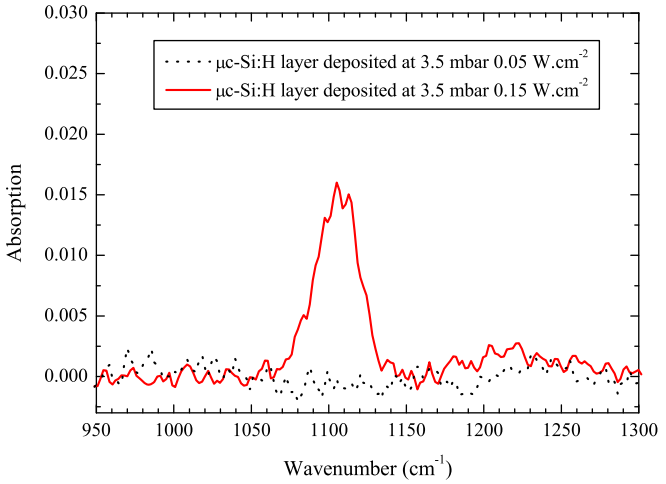


**Fig. 1.** IR spectrum of 600 nm $\mu c-$Si : H films deposited on single-side polished *c*-Si at 0.05 W cm$^{-2}$ and 0.15 W cm$^{-2}$.

Time resolved OES suggests that the ratio of hydrogen to silane radicals flowing to the growth surface increases upon increasing the power density from 0.05 to 0.10 and 0.15 W cm$^{-2}$ with $H_\alpha$/SiH ratio going from 0.06 to 0.10 and 0.12 respectively, while electron temperature remains constant. This might be an indication that a change in the plasma chemical composition is involved in the deterioration of the $\mu c-$Si : H material properties. However, modifications of surface reactions on the growing film cannot be excluded.

### 3.2. IR spectroscopy

Main chemical bonding differences of the deposited $\mu c-$Si : H material was tentatively evaluated with FTIR spectroscopy right after the depositions. Preliminary results show that no significant differences could be made between the low and high power deposition regimes in terms of hydride stretching modes (which may be due to insufficient thickness and signal). In particular we could not identify the signature of narrow high hydride stretching modes, characteristic of hydrogenated crystalline grain boundaries and poor electronic properties [11]. However strong Si–O–Si stretching modes (around 1100 cm$^{-1}$) were observed for the layer deposited at 0.15 W cm$^{-2}$ and completely absent at 0.05 W cm$^{-2}$ (Fig. 1), indicating a porous material associated with

post-deposition oxidation. Nonetheless, further analyses may be necessary to confirm these results. Also a relative increase of bonded hydrogen content of 19% is observed by integrating the wagging mode at 640 $cm^{-1}$ (going from 4.0% to 4.8% in absolute value).

### 3.3. Stress measurements

Stress measurements were carried out by depositing $\mu c$–Si : H layers using the aforementioned deposition regimes with increasing power density, as well as other ones with varying pressure or $H_2$ flow rate detailed in Table 1. The same microcrystalline *p*-layer used within the solar cell devices was systematically deposited before the *i*-layer to be analyzed, and is included within the total thickness of 300 nm common to all these samples. The intrinsic compressive stress has been measured in these films and are shown in Fig. 2. We report here varying intrinsic stress values depending on the deposition conditions for the same crystalline fraction. The differences observed here may be ascribed to varying hydrogen inclusion within the layer, either in clustered (Si–$H_x$) or molecular ($H_2$) forms [12]. For the deposition done at 0.10 W $cm^{-2}$ reducing the hydrogen flow rate, and adapting the silane flow rate for obtaining same $R_c$, the stress in the film decreased from 649 to 600 MPa. The most remarkable decrease was observed at 0.15 W $cm^{-2}$, by increasing the pressure up to 7.0 mbar where it drops from 678 to 481 Mpa. Both regimes are associated with increased silane depletion which was already identified as an important factor for material quality [13].

### 3.4. HFS (ERDA)—absolute H content

Total H content was also evaluated by hydrogen forward scattering spectrometry (HFS), which has the advantage over FTIR evaluation that not only bonded H is measured but non-bonded H as well. A relative increase of H content of 26% is observed between the low and the high power regime (from 8.7% to 11% in absolute value), but for the regime at 0.10 W $cm^{-2}$ with lower hydrogen flow rate, a "high" value close to 11% is also observed although the stress is lowered. Thus, although H content may influence the intrinsic stress of $\mu c$–Si : H layers, there is no clear correlation between them.

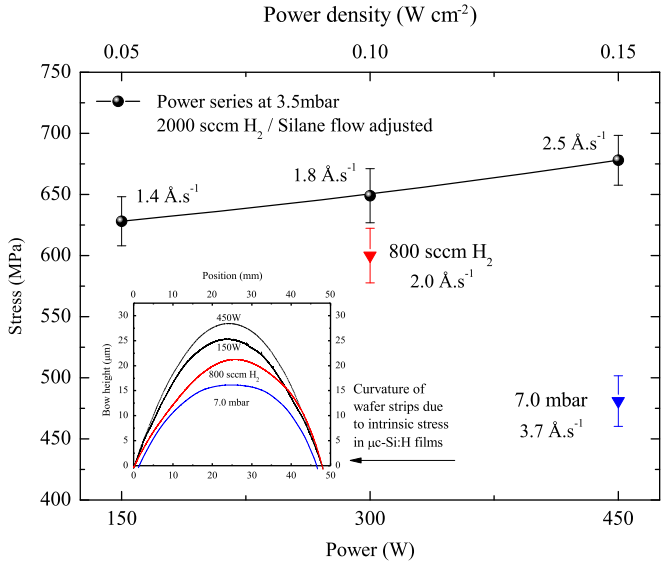


**Fig. 2.** Intrinsic stress in $\mu c$–Si : H films deposited on Si(1 0 0) wafer strips with various deposition parameters. Inset: surface profiles of wafer strips bending as measured with profilometer.

## 4. Microcrystalline and micromorph solar cells

Single junction *p-i-n* $\mu c$–Si : H solar cells with their absorber layer deposited using the new high depletion regimes previously discussed in Section 3.3 and detailed in Table 1 were prepared as well. It can be seen from Fig. 3 that these regimes, which induce lower stress in the material, also lead to higher efficiency devices, mainly through improved $V_{oc}$ and FF. Device-grade $\mu c$–Si : H material is obtainable at a higher pressure of 7.0 mbar, with high open circuit voltages above 520 mV and fill factors above 74%. The best cell performances obtained were $V_{oc}$ = 535 mV, FF = 74.6%, $J_{sc}$ = 19.7 mA $cm^{-2}$ and 7.9% efficiency.

When used as a bottom cell of a micromorph tandem cell, using an *a*-Si:H top cell developed in a KAI reactor as well, the fabrication of a 1.2 $cm^2$ micromorph device with 12.3% initial efficiency, with $V_{oc}$ = 1.33 V, FF = 72.4% and $J_{sc}$ = 12.8 mA $cm^{-2}$ was achieved. Intrinsic layer thicknesses were 250 nm and 2.7 µm for top and bottom cells respectively. A SiO-based intermediate reflector deposited in the same reactor and a broadband anti-reflective coating on glass were used to achieve this result. Both initial and degraded state electrical performances of the device are presented in Fig. 4. After 1000 h of light soaking,

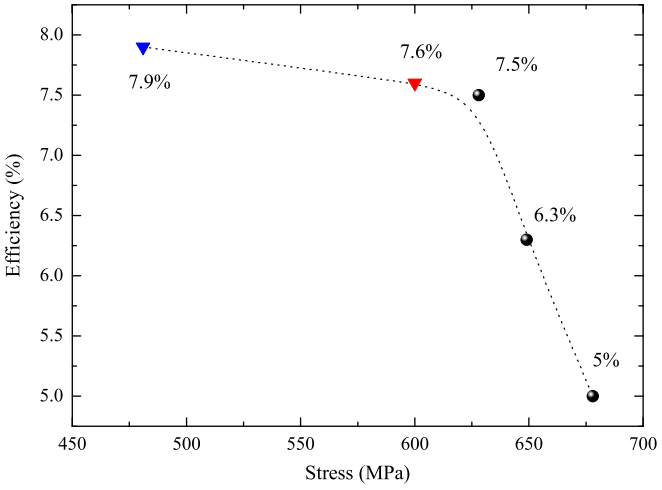


**Fig. 3.** Best efficiencies of 1 µm thick *p-i-n* $\mu c$–Si : H solar cell as a function of their absorber layer intrinsic stress associated to the deposition regime used (detailed in Table 1).

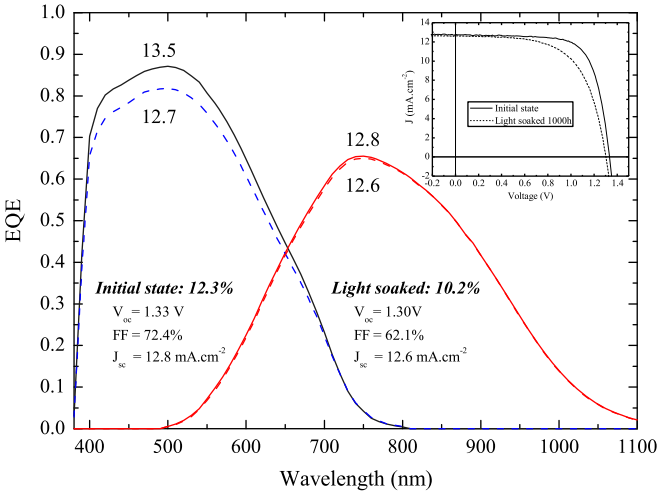


**Fig. 4.** EQE and IV curves (inset) of a micromorph *p-i-n* device at initial (plain line) and degraded (dashed line) states.

Please cite this article as: G. Bugnon, et al., Sol. Energy Mater. Sol. Cells (2010), doi:10.1016/j.solmat.2010.05.014

the device has a relative degradation value of 17%. This suggests that further improvements can be expected for both top and bottom cells in terms of $V_{oc}$ and $J_{sc}$ in particular for stabilized state.

## 5. Conclusion

In this study $\mu c-$Si : H material quality was evaluated in a large area industrial deposition system with combined plasma diagnostic techniques and material characterization. Intrinsic stress of the deposited films was quantified, and various plasma deposition parameters were varied trying to reduce the observed stress. Namely, in the range of our study, increased pressure and reduced hydrogen flow rate during deposition could reduce it, whereas higher power densities tend to increase it. Preliminary results on the origin of stress are discussed and in particular the role of hydrogen. Low stress induced deposition regimes allowed for the fabrication of better performing solar cell devices when used for the deposition of the absorber layer. Based on these results high efficiency single junction $\mu c-$Si : H and micromorph solar cell devices were prepared.

## References

[1] B. Strahm, A.A. Howling, L. Sansonnens, C. Hollenstein, Plasma silane concentration as a determining factor for the transition from amorphous to microcrystalline silicon in SiH4/H2 discharges, Plasma Sources Science and Technology 16 (1) (2007) 80–89, URL: 〈http://stacks.iop.org/0963-0252/16/80〉.

[2] H. Fujiwara, M. Kondo, A. Matsuda, Stress-induced nucleation of microcrystalline silicon from amorphous phase, Japanese Journal of Applied Physics 41 (Part 1, No. 5A) (2002) 2821–2828, doi:10.1143/JJAP.41.2821 URL: 〈http://jjap.ipap.jp/link?JJAP/41/2821/〉.

[3] J. Perrin, J. Schmitt, C. Hollenstein, A.A. Howling, L. Sansonnens, The physics of plasma-enhanced chemical vapour deposition for large-area coating: industrial application to flat panel displays and solar cells, Plasma Physics and Controlled Fusion 42 (12B) (2000) B353–B363 URL: 〈http://stacks.iop.org/0741-3335/42/B353〉.

[4] R. Bartlome, A. Feltrin, C. Ballif, Infrared laser-based monitoring of the silane dissociation during deposition of silicon thin films, Applied Physics Letters 94 (20) (2009) 201501-1–201501-3 , doi:10.1063/1.3141520 URL: 〈http://link.aip.org/link/?APL/94/201501/1〉.

[5] U. Fantz, Spectroscopic diagnostics and modelling of silane microwave plasmas, Plasma Physics and Controlled Fusion 40 (6) (1998) 1035–1056 URL: 〈http://stacks.iop.org/0741-3335/40/1035〉.

[6] A.A. Howling, B. Strahm, P. Colsters, L. Sansonnens, C. Hollenstein, Fast equilibration of silane/hydrogen plasmas in large area RF capacitive reactors monitored by optical emission spectroscopy, Plasma Sources Science and Technology 16 (4) (2007) 679–696 URL: 〈http://stacks.iop.org/0963-0252/16/679〉.

[7] E. Vallat-Sauvain, C. Droz, F. Meillaud, J. Bailat, A. Shah, C. Ballif, Determination of Raman emission cross-section ratio in hydrogenated microcrystalline silicon, Journal of Non-Crystalline Solids 352 (9–20) (2006) 1200–1203 URL: 〈http://www.sciencedirect.com/science/article/B6TXM-4JRKWV2-1/2/2021fc7bb2a907b0f8b41e5f44a9ee76〉.

[8] A. Brenner, S. Senderoff, Calculation of stress in electrodeposits from the curvature of a plated strip, Journal of Research of the National Bureau of Standards 42 (2) (1949) 105–123.

[9] W.A. Brantley, Calculated elastic constants for stress problems associated with semiconductor devices, Journal of Applied Physics 44 (1) (1973) 534–535, doi:10.1063/1.1661935 URL: 〈http://link.aip.org/link/?JAP/44/534/1〉.

[10] J. Bailat, D. Domine, R. Schluchter, J. Steinhauser, S. Fay, F. Freitas, C. Bucher, L. Feitknecht, X. Niquille, T. Tscharner, A. Shah, C. Ballif, High-efficiency p-i-n microcrystalline and micromorph thin film silicon solar cells deposited on lpcvd zno coated glass substrates, in: Conference Record of the 2006 IEEE 4th World Conference on Photovoltaic Energy Conversion, vol. 2, 2006, pp. 1533–1536. URL: 〈http://dx.doi.org/10.1109/WCPEC.2006.279775〉 doi:10.1109/WCPEC.2006.279775.

[11] A.H.M. Smets, T. Matsui, M. Kondo, High-rate deposition of microcrystalline silicon p-i-n solar cells in the high pressure depletion regime, Journal of Applied Physics 104 (3) (2008) 034508-1–034508-11, doi:10.1063/1.2961334 URL: 〈http://link.aip.org/link/?JAP/104/034508/1〉.

[12] U. Kroll, J. Meier, A. Shah, S. Mikhailov, J. Weber, Hydrogen in amorphous and microcrystalline silicon films prepared by hydrogen dilution, Journal of Applied Physics 80 (9) (1996) 4971–4975, doi:10.1063/1.363541 URL: 〈http://link.aip.org/link/?JAP/80/4971/1〉.

[13] G. Bugnon, A. Feltrin, F. Meillaud, J. Bailat, C. Ballif, Influence of pressure and silane depletion on microcrystalline silicon material quality and solar cell performance, Journal of Applied Physics 105 (6) (2009) 064507-1–064507-7, doi:10.1063/1.3095488 URL: 〈http://link.aip.org/link/?JAP/105/064507/1〉.

Please cite this article as: G. Bugnon, et al., Sol. Energy Mater. Sol. Cells (2010), doi:10.1016/j.solmat.2010.05.014